An Incremental Block-Line-Gauss-Seidel Method for the Navier-Stokes Equations

M. Napolitano*
Università di Bari, Bari, Italy
and
R. W. Walters†
NASA Langley Research Center, Hampton, Virginia

A block-line-Gauss-Seidel (LGS) method is developed for solving the incompressible and compressible Navier-Stokes equations in two dimensions. The method requires only one block-tridiagonal solution process per iteration and is consequently faster per step than the linearized block-alternating-direction-implicit (ADI) methods. Results are presented for both incompressible and compressible separated flows: in all cases the proposed block-LGS method is more efficient than the block-ADI methods. Furthermore, for high-Reynolds-number weakly separated incompressible flow in a channel, which proved to be an impossible task for a block-ADI method, solutions have been obtained very efficiently using the new scheme.

Introduction

THIS paper provides a simple and efficient numerical technique for solving incompressible and compressible two-dimensional viscous flow problems, including separation effects, particularly at moderate-to-high Reynolds numbers. It is well known that for high-Reynolds-number viscous flows, the CFL stability condition of explicit schemes results in a severe time-step limitation, so that they are computed more conveniently using implicit methods. However, fully implicit schemes require the extremely costly, if even feasible, inversion of a different large, sparse matrix at every iteration. Therefore, in the last decade, the most successful and widely used methods for solving compressible viscous flows have been the so-called "linearized block-alternating-direction-implicit" (block-ADI) methods of Beam and Warming[1] and Briley and McDonald.[2,3] The time-dependent, compressible Navier-Stokes equations are discretized and linearized in time using the Taylor series expansion and solved numerically by means of an ADI method of the Douglas-Gunn[4] type, which requires the solution of block-tridiagonal systems only.

The same idea has also been applied with some success to the vorticity-stream function incompressible Navier-Stokes equations[5-7]: the stream function is parabolized in time using a relaxation-like time derivative[8] and solved coupled with the vorticity transport equation using a linearized block-ADI method. Among the many desirable features of block-ADI methods, it is noteworthy that the incremental (delta) approach of Ref. 1 allows straightforward use of different discretizations such as first-order-accurate upwind differences in the implicit operator and second-order-accurate central differences in the right-hand side (RHS).[7] Artificial viscosity is thus introduced into the (false) transient to enhance the method's stability and convergence rate, but a second-order-accurate, steady-state solution is recovered at convergence. However, schemes of the ADI type have two major limitations: their convergence rate deteriorates very rapidly for values of the time step different from the optimal one,[9] and also as the Reynolds number increases.

The aim of this investigation is to show that both limitations can be overcome by a numerical technique that is just as simple as the aforementioned ADI methods.[1-6]

It has been shown in Refs. 10 and 11 that, in connection with upwind discretizations of the Euler equations, classical point and line Gauss-Seidel relaxation methods converge much faster than approximate factorization methods of the ADI type for both two- and three-dimensional subsonic and transonic flows. The apparent reason for the improvement is the use of two-point upwind differences for the advective terms in the implicit operator leading to the solution of an algebraic system characterized by a diagonally dominant coefficient matrix suitable for solution by means of relaxation methods. The same situation arises when dealing with the Navier-Stokes equations, therefore, it is reasonable to anticipate that a LGS method using the delta approach[1] and upwind differences for the advective terms in the implicit operator will outperform ADI methods also for the case of viscous flows. In particular, for the case of high-Reynolds-number weakly separated flows of practical interest (when the so-called thin-layer equations are valid), the problem is only weakly elliptic in the streamwise direction due to upstream pressure influence in the separation region. Therefore, a LGS method that accounts for the influence across the boundary layer as well as for the downstream influence, implicitly, and

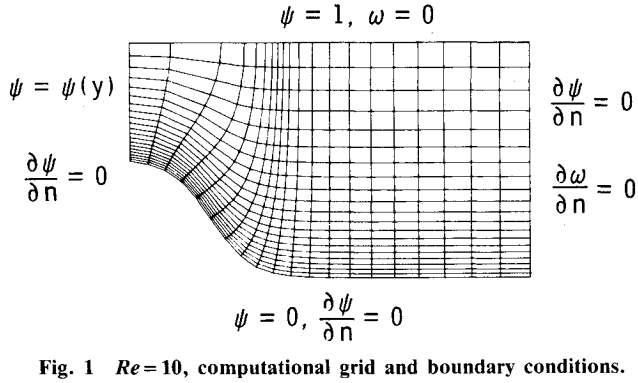

Fig. 1 $Re = 10$, **computational grid and boundary conditions.**

Received Dec. 24, 1984; presented as Paper 85-0033 at the AIAA 23rd Aerospace Sciences Meeting, Reno, NV, Jan. 14-17, 1985; revision received June 15, 1985. This paper is declared a work of the U.S. Government and is not subject to copyright protection in the United States.

*Professor, Istituto di Macchine. Member AIAA.
†National Research Council Research Associate; presently Assistant Professor, Virginia Polytechnic Institute and State University. Member AIAA.

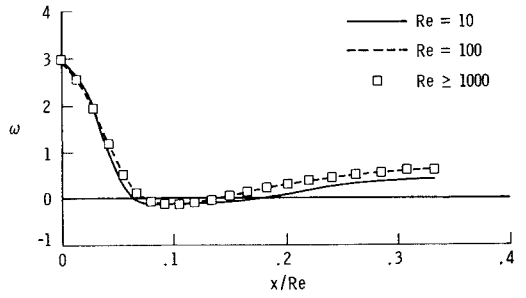

Fig. 2 Wall vorticity distribution for various values of the Reynolds number.

iterates in time to account for the weak upstream influence, is likely to be more efficient than the block-ADI methods.

Such a numerical technique is provided herein for both the vorticity-stream function equations and the compressible Navier-Stokes equations in conservation form. Numerical results are presented for rather difficult high-Reynolds-number separated flows which demonstrate the superior efficiency and robustness of the proposed method with respect to the block-ADI methods.

Incompressible Flow

Numerical Technique

The parabolized, nondimensional, vorticity-stream function equations in a general curvilinear coordinate system are given as

$$\omega_t + (\psi_\eta\omega_\xi - \psi_\xi\omega_\eta)/J - (\alpha\omega_{\xi\xi} - 2\beta\omega_{\xi\eta} + \gamma\omega_{\eta\eta} + \sigma\omega_\eta + \tau\omega_\xi)/Re = 0 \quad (1)$$

$$\psi_t - (\alpha\psi_{\xi\xi} - 2\beta\psi_{\xi\eta} + \gamma\psi_{\eta\eta} + \sigma\psi_\eta + \tau\psi_\xi) - \omega = 0 \quad (2)$$

In Eqs. (1) and (2), Re is the Reynolds number, ω and ψ indicate the vorticity and stream function, respectively, t the time, ξ and η the general body-oriented curvilinear coordinates,[12] and J, α, β, γ, σ, and τ are the Jacobian and scale factors of the coordinate transformation $(x,y \rightarrow \xi,\eta)$, whose expressions are given in Ref. 12.

Equations (1) and (2) are discretized in time by a two-level implicit Euler scheme and linearized using the delta (Δ) approach,[1] by neglecting terms of order Δ^2, to give

$$\frac{\Delta\omega}{\Delta t} + \frac{1}{J}[\psi^n_\eta\Delta\omega_\xi + \omega^n_\xi\Delta\psi_\eta - \psi^n_\xi\Delta\omega_\eta - \omega^n_\eta\Delta\psi_\xi] - \frac{1}{Re}(\alpha\Delta\omega_{\xi\xi} + \gamma\Delta\omega_{\eta\eta} + \sigma\Delta\omega_\eta + \tau\Delta\omega_\xi) = -\frac{1}{J}(\psi^n_\eta\omega^n_\xi - \psi^n_\xi\omega^n_\eta) + \frac{1}{Re}(\alpha\omega^n_{\xi\xi} - 2\beta\omega^n_{\xi\eta} + \gamma\omega^n_{\eta\eta} + \sigma\omega^n_\eta + \tau\omega^n_\xi) \quad (3)$$

$$\frac{\Delta\psi}{\Delta t} - (\alpha\Delta\psi_{\xi\xi} + \gamma\Delta\psi_{\eta\eta} + \sigma\Delta\psi_\eta + \tau\Delta\psi_\xi) - \Delta\omega = (\alpha\psi^n_{\xi\xi} - 2\beta\psi^n_{\xi\eta} + \gamma\psi^n_{\eta\eta} + \sigma\psi^n_\eta + \tau\psi^n_\xi) + \omega^n \quad (4)$$

where Δt is the time step and $\Delta\omega = \omega^{n+1} - \omega^n$, where the superscripts $n+1$ and n indicate the new and old time levels $t^{n+1} = t^n + \Delta t$ and t^n, etc. Notice that the mixed-type derivatives are evaluated at the old time level t^n; i.e., explicitly and therefore do not appear in delta form. However, this is of no consequence when using an orthogonal coordinate system ($\beta \equiv 0$), as in this study.

Equations (3) and (4) are discretized in space using two-point, first-order-accurate upwind differences for the first derivatives of the incremental variables in Eq. (3) and second-order-accurate central differences for all of the other terms to provide, together with appropriate boundary conditions, a large linear system of the type

$$\underline{\underline{A}}f = b \quad (5)$$

where $\underline{\underline{A}}$ is a large 2×2 block-pentadiagonal matrix, b is a known vector, and f is the unknown vector whose elements are the two-element vectors $(\Delta\omega, \Delta\psi)^T$ evaluated at every grid-point location.

In Ref. 7, the system given by Eq. (5) was factorized and solved approximately by a two-sweep block-ADI method. Here, the uppermost diagonal of matrix A (corresponding to the downstream point in the standard five-point computational stencil) is dropped; Eq. (5) is thus solved approximately as a series of 2×2 block-tridiagonal systems, bringing the lowest diagonal entries to the right-hand side. The solution is then updated to read

$$(\omega^n, \psi^n)^T \leftarrow (\omega^n, \psi^n)^T + (\Delta\omega, \Delta\psi)^T \quad (6)$$

and the process is repeated until convergence is obtained. It is noteworthy that, for flows having a strong elliptic character (e.g., the driven cavity flow[13]), a different ordering for matrix A is used at every other time step, so as to implicitly account for all of the points of the computational stencil except the lowest one.

Regarding the boundary conditions, the double specification for the stream function at the body surface can be implemented straightforwardly using the point-image technique of Burggraf.[13] The steady-state form of the stream function equation is used at the boundary grid point to eliminate the additional unknown (i.e., the stream function at the point image) and to evaluate the vorticity at the boundary directly from the solution of the 2×2 block-tridiagonal system.[6,7] On the first and last lines of the computational grid, after imposing the Dirichlet condition for $\Delta\psi$, $\Delta\omega$ is evaluated explicitly using the Neumann condition for ψ and again the steady-state stream function equation to eliminate the unknown point-image value of $\Delta\psi$.

Results

In order to test the proposed methodology, two very different problems have been considered for which the block-ADI method of Ref. 7 has been found to be very satisfactory at moderate values of the Reynolds number but has encountered severe difficulties at higher Re.

The first problem is the weakly separated channel flow proposed by Roache.[14] The geometry of the channel, together with the appropriate boundary conditions and the coordinates employed in Ref. 7, are given in Fig. 1 for $Re = 10$. Roache has shown that, if the length of the channel is increased proportionally to Re, for $Re \gg 1$, the solution takes on a quasi-self-similar form (see Fig. 2). As such, the present problem is very suitable to assess the capability of a given numerical method to compute weakly separated flows at high Reynolds numbers. For $Re = 10$ and 100, the block-ADI method was found to be extremely efficient[7]; however, for $Re > 100$ its convergence rate deteriorated rapidly, and for $Re \geq 10^4$ a converged solution could not be obtained at any cost. The present method, employing the same coordinate transformation and spatial discretization as used in Ref. 7, has been applied to compute solutions for $Re = 10, 10^2, \ldots, 10^{15}$. Convergence to machine accuracy (residual $< 10^{-6}$) has been obtained on a 21×21 grid in less than 60 iterations (time cycles), which amounts to less than 1 min of CPU time on a Hewlett-Packard 9000/9040A

minicomputer, by using a value of the time step initially equal to Re and increasing it with the inverse of the residual during the solution process. For the case $Re = 10^{15}$ the final time step was as high as 10^{21}, verifying the unconditional stability of the method. Such an unconditional stability is probably due to the viscous nature of the flow. In fact, the present algorithm is not unconditionally stable for the case of a linear scalar advection equation (see the Appendix), but can be easily modified to achieve unconditional stability. This channel problem obviously has a weaker and weaker elliptic nature with increasing Re, so that it comes as no surprise that the present LGS method, marching from upstream to downstream, is almost as efficient as a fully implicit method using the same linearization procedure.

A rather difficult problem that has a strong elliptic nature, namely, the driven cavity flow at $Re \geq 10^3$, has also been considered to test the performance of the proposed method vs the corresponding ADI technique.[5-7] The analytical stretching used in Ref. 6 has been employed to transform a suitable nonuniform grid in the physical x,y plane into a uniform grid in the computational ξ,η plane, according to the following transformation:

$$\begin{pmatrix} x \\ y \end{pmatrix} = 0.5 + 0.5\tanh\left[1.8\begin{pmatrix} 2\xi - 1 \\ 2\eta - 1 \end{pmatrix}\right] \Big/ \tanh(1.8) \qquad (7)$$

Solutions have been obtained for $Re = 10^3$ using 21×21, 31×31, and 41×41 equally spaced grid points in the ξ,η plane and evaluating all of the scale factors of the coordinate transformation numerically to second-order accuracy everywhere. The two coarsest mesh solutions obviously coincide with those obtained by using the ADI method[7] but required less than one-fifth of the iterations and, therefore, less than one-tenth of the computer time to converge to machine accuracy using a nonoptimized unitary time step; the finest grid solution, which was too costly to obtain in Ref. 7, required only about 600 iterations corresponding to 30 min of CPU time on the aforementioned minicomputer. The stream function contours are given in Fig. 3 and are found to be very similar to the accurate contours due to Ghia et al.[15]

It is noteworthy to mention that the use of the delta formulation[1] allows the use of different discretizations in the right-hand sides of Eqs. (3) and (4), which control the accuracy of the solution, without modifying the left-hand side (LHS); i.e., the structure of matrix A. In particular for the case of uniform grids, it has been shown in Ref. 16 that a considerable improvement in accuracy is obtained by writing the advection terms in Eq. (1) in conservation form; i.e., as

$$[(\psi_\eta \omega)_\xi - (\psi_\xi \omega)_\eta]/J \qquad (8)$$

Solutions have thus been obtained by approximating the advection terms in the RHS of Eq. (3) according to a second-order-accurate central difference discretization of Eq. (8). The computed maximum grid-point value for the stream function $|\psi|_M$ and the value of the vorticity at the center of the moving wall ω_c are given in Table 1 together with the standard method results and the very accurate solution of Ghia et al.[15] A marked accuracy improvement is obtained. Furthermore, it is noteworthy that using such a discretization was found to improve the convergence rate of the numerical technique by about 10%.

A third-order-accurate approximation for the Neumann boundary condition at the wall has also been implemented so as to evaluate the vorticity at the wall to second-order accuracy.[15] To this purpose, the boundary condition treatment described in Ref. 15 has been generalized to the present case of a nonuniform grid. The results are also given in Table 1, where they appear markedly more accurate than those ob-

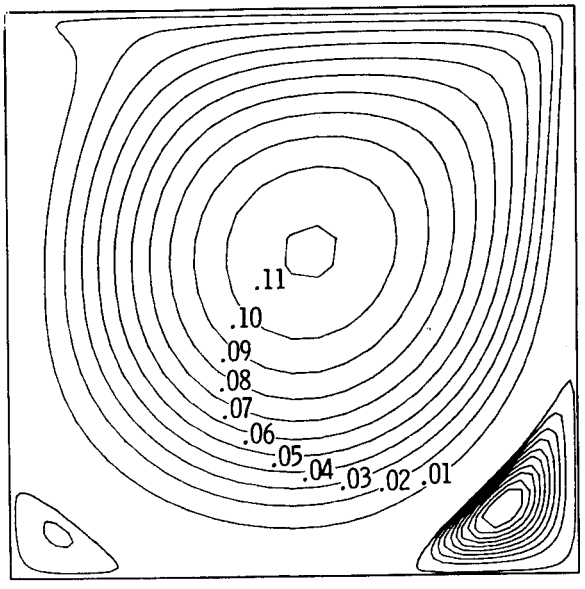

Fig. 3 Stream function contours, $|\psi|$, for $Re = 1000$ test case.

Table 1 Driven cavity results

Mesh	Standard	Conservative	Second-order boundary condition
Computed values of $\|\psi\|_M$ for $Re = 10^3$; exact value = 0.1179			
21×21	0.0913	0.1085	0.1126
31×31	0.1055	0.1144	0.1160
41×41	0.1110	0.1164	0.1172
Computed values of ω_c for $Re = 10^3$; exact value = 14.890			
21×21	17.29	13.26	15.035
31×31	15.92	14.13	14.969
41×41	15.47	14.41	14.896

Comparison of exact and computed results (41×41 grid, second order boundary conditions) for the $Re = 3200$ test case

	Computed	Exact
$\|\psi\|_M$	0.1184	0.1204
ω_c	25.92	25.39

tained using the less accurate boundary condition, especially for the coarsest 21×21 mesh.

In order to better assess the adequacy of the present 41×41 mesh solutions, the u and v velocity profiles along the vertical and horizontal midplanes of the cavity have been plotted in Fig. 4 for both the standard and conservative approximations of the advection terms. Both solutions are reasonably close to each other and the conservative solution is seen to practically coincide with that of Ref. 15.

The $Re=3200$ flow case was finally considered as a very severe test for the present method. A solution was obtained using a 41×41 mesh, with the conservative form of the advection terms and the second-order-accurate boundary conditions; however, the time step in the vorticity equation has to be reduced to 0.2 in order to avoid divergence and about 3000 iterations were necessary for the solution to converge to machine accuracy. The results for $|\psi|_M$ and ω_c are again given in Table 1 where they are seen to compare very favorably with those of Ref. 15, especially considering that a relatively coarse mesh has been employed to resolve a very complicated flowfield.

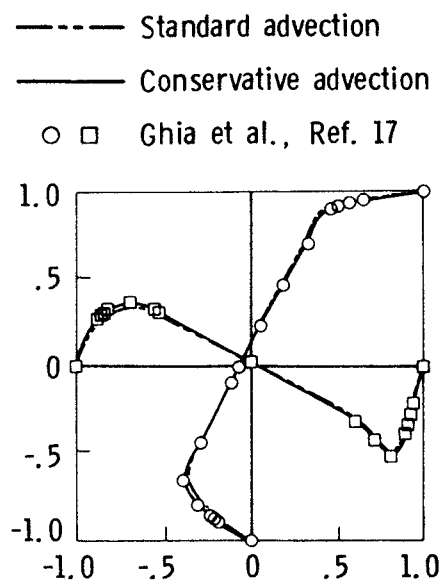

Fig. 4 Velocity components along the vertical and horizontal midplanes.

Compressible Flow

Numerical Technique

The two-dimensional, compressible Navier-Stokes equations in conservation form are given in generalized coordinates as

$$\frac{\partial q}{\partial t}+\frac{\partial E}{\partial \xi}+\frac{\partial F}{\partial \eta}=Re^{-1}\left(\frac{\partial V}{\partial \xi}+\frac{\partial S}{\partial \eta}\right) \tag{9}$$

where $q=[\rho,\ \rho u,\ \rho v,\ e]^T/J$ and E, F, V, and S are the flux vectors associated with the inviscid and viscous terms. Application of the implicit Euler time integration scheme, time linearization, spatial discretization, and the delta form[1] results in

$$\left[\frac{I}{\Delta t}+\nabla_\xi A^+ +\Delta_\xi A^- +\nabla_\eta B^+ +\Delta_\eta B^- -\frac{1}{Re}(\bar\delta_\xi N+\bar\delta_\eta M)\right]\Delta q=-\left[\delta_\xi E+\delta_\eta F-\frac{1}{Re}(\bar\delta_\xi V+\bar\delta_\eta S)\right]^n \tag{10}$$

where the subscripted ∇ and Δ are the first-order-accurate backward and forward difference operators for the first derivative, δ the second-order-accurate central difference operator for the first derivative, and $\bar\delta$ the standard second-order difference operator for the viscous terms.

The RHS of Eq. (10) has been discretized using central differences, whereas the "upwinding" of the implicit convective terms in the LHS is based on van Leer's continuously differentiable flux vector splitting procedure for the Euler equations.[17] In order to compute flows with shocks, the classic fourth-order dissipation has been added to the RHS in the form

$$-\frac{\alpha}{J}[(\nabla\Delta)^2_\xi+(\nabla\Delta)^2_\eta]Jq \tag{11}$$

The Van Leer flux vector splitting was chosen for the LHS of Eq. (10) because it has the advantages of simplicity, smoothness through sonic points, and yields a well-conditioned linear system amenable to the LGS relaxation process. This last property should be stressed since it results in an algorithm that converges for arbitrarily large Courant numbers as opposed to the spatially split central difference schemes which fail to converge for sufficiently large time steps. Furthermore, for convection-dominated problems, the ADI schemes have a small range of time steps for which rapid convergence is obtained,[9] and which varies from problem to problem thus detracting from the versatility of the method. This difficulty is overcome with the present method in which the same time-stepping strategy is effective for all problems considered to date.

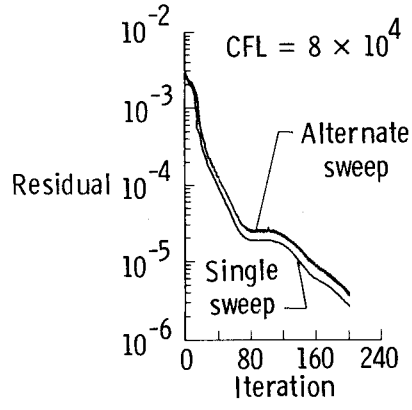

Fig. 5 Convergence history comparison for shock/boundary-layer interaction problem.

The Jacobian matrices associated with the linearization of the convective fluxes in a generalized coordinate system are formed using the approach of Anderson et al.,[18] which will be briefly reviewed here for completeness.

Let T be a rotation matrix given by

$$T=\frac{1}{|\nabla\xi|}\begin{bmatrix}|\nabla\xi| & 0 & 0 & 0\\ 0 & \xi_x & \xi_y & 0\\ 0 & -\xi_y & \xi_x & 0\\ 0 & 0 & 0 & |\nabla\xi|\end{bmatrix} \tag{12}$$

where $\nabla\xi=\text{grad}\xi$, and let

$$\tilde q=Tq=J^{-1}\begin{bmatrix}\rho\\ \rho\tilde u\\ \rho\tilde v\\ e\end{bmatrix};\quad \tilde E=TE=\frac{|\nabla\xi|}{J}\begin{bmatrix}\rho\tilde u\\ \rho\tilde u^2+p\\ \rho\tilde u\tilde v\\ (e+p)\tilde u\end{bmatrix} \tag{13}$$

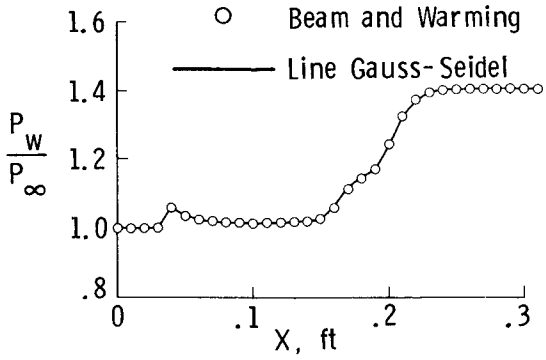

Fig. 6 Pressure distribution at the wall.

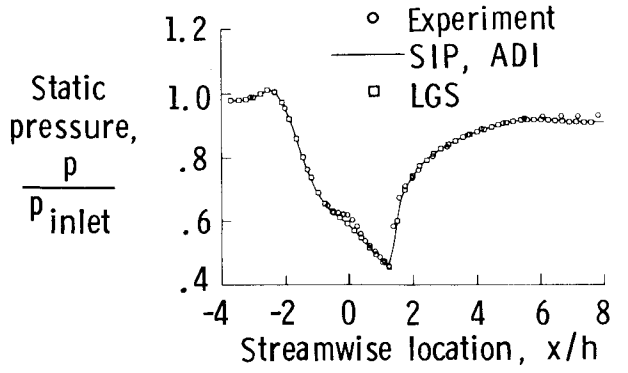

Fig. 7 Experimental and predicted pressure distribution along the top wall of the diffuser.

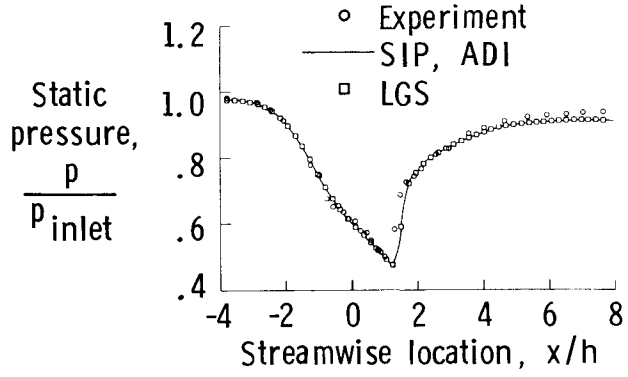

Fig. 8 Experimental and predicted pressure distribution along with bottom wall of the diffuser.

Here, $\bar{u}=(\xi_x u+\xi_y v)/|\nabla\xi|$ and $\bar{v}=(-\xi_y u+\xi_x v)/|\nabla\xi|$ represent the velocities normal and tangential to the lines of constant ξ. The rotated flux $\bar{E}$ is now of the same form as the flux in a Cartesian system and, therefore, can be split according to the original van Leer decomposition.[17] Thus, the generalized split fluxes are

$$E^{\pm}=T^{-1}\bar{E}^{\pm} \tag{14}$$

and similarly for $F^{\pm}$.

The Jacobian matrices can finally be formed by straightforward chain-rule differentiation; e.g.,

$$A^{+}=\frac{\partial E^{+}}{\partial q}=\frac{\partial(T^{-1}\bar{E}^{+})}{\partial\bar{q}}\frac{\partial\bar{q}}{\partial q}=T^{-1}\frac{\partial\bar{E}^{+}}{\partial\bar{q}}T \tag{15}$$

Linearization of the viscous terms is performed in the usual manner[19] and will not be repeated here.

The solution strategy of the linear system is the same as that employed for the ψ,ω equations; the main difference being the block size. After each iteration, the solution is updated by $q^{n+1}=q^n+\Delta q$ and the entire procedure is repeated until convergence.

A different value of the time step is employed at every iteration level, namely

$$\Delta t=\frac{\Delta t_0}{\|R\|_2^n} \tag{16}$$

where $\|R\|_2^n$ is the L_2 norm of the RHS of Eq. (10) normalized by the initial residual and Δt_0 is the initial time step. Δt_0 is chosen such that the maximum Courant number at the outset of the calculation is between 10 and 20, allowing the initial solution to adjust itself to the enforcement of the steady-state boundary conditions without incurring severe oscillations. When freestream conditions are chosen as the initial guess, as done here, the residual usually drops very rapidly so that a quite large Courant number is obtained after only a few iterations.

Results

Several test problems have been computed that are described in detail elsewhere in the literature. The first and simplest is the well-known shock/boundary-layer interaction problem in which a shock wave of prescribed strength interacts with a laminar boundary layer developing on a flat plate. The details of the problem, the boundary condition treatment, and the mesh are identical to those described in Refs. 1 and 19.

Results were obtained using the proposed method and two different marching strategies, for which the convergence histories are displayed in Fig. 5. The curve labeled "single sweep" was obtained by passing through the mesh in a left-to-right fashion using vertical LGS at every iteration. The curve labeled "alternate sweep" was obtained, instead, by using a right-to-left pass through the mesh at every other iteration. Since adverse waves are present in the boundary layer, one might have expected the single-sweep procedure to give rise to an instability (see the Appendix). Evidently, the presence of viscous effects is sufficient to stabilize the single-sweep method. In fact, no underrelaxation was necessary in either computation, although the maximum Courant number was as high as 80,000. The converged results are given in Fig. 6 as the pressure distribution ahead of and on the plate for both the LGS method (solid line) and the Beam and Warming algorithm (symbols). As is obvious, all methods converge to the same steady-state solution, independent of the time step.

A second case of turbulent flow in the terminal shock region of an inlet/diffuser was considered as a severe test for the present method. This problem has been studied extensively, both experimentally[20] and numerically.[19,21-23] The flow is transonic and only quasisteady, insofar as nondecaying, small, self-induced oscillations associated with the terminal shock are present; the mean shock location and strength are, however, well defined. The inflow Mach number is 0.46 and the Reynolds number based on the nozzle length is 5.865×10^6. The algebraic eddy-viscosity model of Baldwin and Lomax[24] and the same grid and boundary conditions described in Refs. 19 and 20 were employed.

The computed pressure distributions along the top and bottom walls using the Strongly Implicit Procedure (SIP),[20] the Beam and Warming algorithm, and the present LGS method are presented in Figs. 7 and 8, together with the experimental data. Alternate sweep marching and underrelaxation were required to obtain a rapid convergence to the quasisteady state due to the presence of strong adverse waves. However, fewer iterations (<300) were required by the present LGS method than by either ADI or SIP, both of which required greater than 500 iterations.[19] In terms of total CPU time, the LGS method required only 53% of the

time required by ADI, whereas SIP required 12% more than the ADI method.

Conclusions

A new method has been developed for solving two-dimensional viscous flows, using the incremental form of the governing equations, a deferred correction upwind strategy, and classical line Gauss-Seidel relaxation. The proposed method has all of the favorable features of the linearized block-ADI methods and, in addition, is more robust insofar as its convergence rate is much less sensitive to the value of the time step. Several results for both incompressible and compressible flows are presented which illustrate the validity of the proposed methodology.

Appendix: Stability Analysis

This appendix is presented to provide insight into the temporal growth/decay properties of the algorithm, especially for the case in which the marching direction is in opposition to the direction of information propagation. This is meant to model, in a rudimentary fashion, the more complicated problem of a system of equations in which there may be both positive and negative traveling characteristics (e.g., subsonic flows). In such a case, the LGS method must always march adverse to at least one of the characteristics. This analysis is not meant to imply that one should march against the flow direction for problems in which all of the characteristics are of the same sign.

Consider the linear scalar advection equation

$$q_t + aq_x = 0, \qquad a > 0 \tag{A1}$$

Writing the difference equation in delta form, using a first-order upwind discretization for the left-hand side, a central difference for the right-hand side, and Euler implicit time integration, yields

$$[1 + \lambda(1 - \beta s^-)]\Delta q = -\lambda(s^+ - s^-)q^n/2 \tag{A2}$$

where

$$\lambda = \frac{a\Delta t}{\Delta x} \quad \text{and} \quad s^{\pm} q_j = q_{j\pm 1}$$

The case $\beta = 1$ corresponds to Gauss-Seidel with left-to-right sweeping (i.e., moving along the characteristic direction) and the $\beta = 0$ case is Gauss-Seidel with right-to-left sweeping (moving adverse to the characteristic direction).

Fourier analysis of Eq. (A2) yields

$$[1 + \lambda(1 - \beta e^{-i\theta})](G - 1) = -\lambda(e^{i\theta} - e^{-i\theta})/2 \tag{A3}$$

or

$$G = \frac{1 + \lambda(1 - \beta\cos\theta) + i\lambda(\beta - 1)\sin\theta}{1 + \lambda(1 - \beta\cos\theta) + i\beta\sin\theta} \tag{A4}$$

for

$$\beta = 1, \quad |G| \le 1$$

$$\beta = 0, \quad |G| \ge 1$$

From the above it can be seen that there are (λ, θ) combinations such that

$$|G|_{\beta=0}\,|G|_{\beta=1} > 1 \tag{A5}$$

implying that the scheme given by Eq. (A2) is not unconditionally stable even when alternating sweep directions are used. However, if $\beta = 0$ is replaced by $\beta = -\phi s^+$ on the right-to-left-sweep, then Fourier analysis gives

$$G_{\beta=-\phi s^+} = 1 - i\left[\frac{\lambda}{1 + \lambda(1 + \phi)}\right]\sin\theta \tag{A6}$$

and though

$$|G|_{\beta=-s^+} > 1 \quad \text{for all } \lambda > 0$$

it is easily shown that

$$|G|_{\beta=1}\,|G|_{\beta=-\phi s^+} \le 1 \quad \text{for all } \lambda > 0 \tag{A7}$$

if

$$\frac{1 + \lambda(1 - \cos\theta)}{1 + \lambda(1 + \phi)} \le 1 \tag{A8}$$

which is satisfied providing

$$\phi \ge 1 \tag{A9}$$

Thus, the scheme given by Eq. (A3) and applied to Eq. (A1) is unconditionally stable if both alternating sweep direction and underrelaxation (with $\phi \ge 1$) are used.

Acknowledgment

This work was supported in part by Ministero Pubblica Istruzione, ONR Grant N00014-82-K-0184 while the first author was visiting Yale University, Department of Computer Science.

References

[1] Beam, R. M. and Warming, R. F., "An Implicit Factored Scheme for the Compressible Navier-Stokes Equations," *AIAA Journal*, Vol. 16, April 1978, pp. 393-402.

[2] Briley, W. R. and McDonald, H., "Solution of the Multidimensional Compressible Navier-Stokes Equations by a Generalized Implicit Method," *Journal of Computational Physics*, Vol. 24, 1977, pp. 372-397.

[3] Briley, W. R. and McDonald, H., "On the Structure and Use of Linearized Block ADI and Related Schemes," *Journal of Computational Physics*, Vol. 24, 1977, pp. 54-73.

[4] Douglas, J. and Gunn, J. E., "A General Formulation of Alternating Direction Methods," *Numerische Mathematik*, Vol. 6, 1964, pp. 428-464.

[5] Hill, J. A., Davis, R. T., and Slater, G. L., "Development of a Factored ADI Scheme for Solving the Navier-Stokes Equations in Stream Function Vorticity Variables," University of Cincinnati, Cincinnati, OH, AFL Rept. 79-17-48, 1979.

[6] Napolitano, M., "Simulation of Viscous Steady Flows Past Arbitrary Two-Dimensional Bodies," *Numerical Methods for Nonlinear Problems*, Pineridge Press, Swansea, U.K., pp. 721-733; also, AFWAL Rept. 80-3038, 1980.

[7] Napolitano, M., "Efficient ADI and Spline ADI Methods for the Steady-State Navier-Stokes Equations," *International Journal for Numerical Methods in Fluids*, Vol. 4, 1984, pp. 1101-1115.

[8] Davis, R. T., "Numerical Solutions of the Navier-Stokes Equations for Symmetric Laminar Incompressible Flow Past a Parabola," *Journal of Fluid Mechanics*, Vol. 51, Pt. 3, 1972, pp. 417-433.

[9] Abarbanel, S. S., Dwoyer, D. L. and Gottlieb, D., "Improving the Convergence Rate of Parabolic ADI Methods," AIAA Paper 83-1897, 1983.

[10] Napolitano, M. and Dadone, A., "Implicit Lambda Methods for Three-Dimensional Compressible Flows," *AIAA Journal*, Vol. 23, Sept. 1985, pp. 1343-1347.

[11] Van Leer, B. and Mulder, W. A., "Relaxation Methods for Hyperbolic Equations," Delft University of Technology, the Netherlands, T.H.D. Rept. 84-20, 1984.

[12] Thompson, J. F., Thames, F. C., and Mastin, C. W., "Boundary-Fitted Curvilinear Coordinate Systems for Solution of Partial Differential Equations on Fields Containing any Number of Arbitrary Two-Dimensional Bodies," NASA CR-2729, 1977.

[13] Burggraf, O. R., "Analytical and Numerical Studies of the Structure of Steady Separated Flows," *Journal of Fluid Mechanics*, Vol. 24, Pt. 1, 1966, pp. 113-151.

[14] Roache, P. J., "Scaling of High Reynolds Number Weakly Separated Channel Flows," Symposium on Numerical and Physical Aspects of Aerodynamic Flows, California State University, Long Beach, CA, Jan. 1981, pp. 1-7.

[15]Ghia, U., Ghia, K. N., and Shin, C.T., "High-*Re* Solutions for Incompressible Flow Using the Navier-Stokes Equations and a Multigrid Method," *Journal of Computational Physics*, Vol. 48, 1982, pp. 387-411.

[16]Rubin, S. G., "Incompressible Navier-Stokes and Parabolized Navier-Stokes Solution Procedures and Computational Techniques," VKI Lecture Series 1982-5, Rhode St. Genese, Belgium, March 1982.

[17]Van Leer, B., "Flux-Vector Splitting for the Euler Equations," *Proceedings of 8th International Conference on Numerical Methods in Fluid Dynamics*, FRG, June 1982.

[18]Anderson, W. K., Thomas, J. L., and van Leer, B., "A Comparison of Finite Volume Flux Vector Splittings for the Euler Equations," AIAA Paper 85-0122, 1985.

[19]Walters, R. W., "*LU* Methods for the Compressible Navier-Stokes Equations," Ph.D. Thesis, North Carolina State University, April 1984.

[20]Bogar, T. J., Sajben, M., and Kroutil, J. C., "Characteristic Frequency and Length Scales in Transonic Diffuser Flow Oscillations," AIAA Paper 81-1291, 1981.

[21]Walters, R. W., Dwoyer, D. L., and Hassan, H. A., "A Strongly Implicit Procedure for the Compressible Navier-Stokes Equations," AIAA Paper 84-0424, 1984.

[22]Liu, N. S., Shamroth, S. J., and McDonald, H., "Numerical Solution of the Navier-Stokes Equations for Compressible Turbulent Two/Three Dimensional Flows in the Terminal Shock Region on an Inlet/Diffuser," AIAA Paper 83-1892, 1983.

[23]Liu, N. S., Shamroth, S. J., and McDonald, H., "Numerical Solutions of Navier-Stokes Equations for Compressible Turbulent Two/Three Dimensional Flows in the Terminal Shock Region of an Inlet/Diffuser," NASA CR-3723, Aug. 1983.

[24]Baldwin, B. S. and Lomax, H., "Thin Layer Approximation and Algebraic Model for Separated Turbulent Flows," AIAA Paper 78-257, Jan. 1978.